Effect of Residual Stresses and Complex Loadings on the Fatigue Behavior of Underclad Cracks

J. L. Bernard, J. Vagner, A. Pellissier-Tanon, F. Faure
FRAMATOME, Paris la Défense, France

ABSTRACT

The objective of this paper is to show that the fatigue crack propagation of cold underclad cracks in reactor vessel nozzles is much less than predicted by usual conservative safety assessment methods, and that it is possible to estimate real margins more accurately.

The crack propagation of underclad cracks was assessed by numerical methods with conservative safety hypotheses :
- upper bounds of fatigue crack propagation laws in air environment have been used for both the base metal and the cladding.
- fatigue crack initiation on the actual underclad defects has not been taken into account.
- crack lengths have been corrected using Irwin's correction which accounts for plastic zone sizes at crack tips.
- elliptical defects have been considered to be strip defects.
- lower bounds of yield strengh and thoughness of the materials have been used.

An extensive experimental fatigue program was also performed on large specimens in several laboratories.
The specimens were taken out of a full size nozzle (SA 508 Cl.3 steel) containing cracks in the heat affected zone under the 3 layers cladding.

The experimental observations are as follows :
- a significant fraction of lifetime is spent in crack initiation.
- the crack growth rate is lower because of a non agressive (inert) environment in the defects.
- residual stresses at 300°C can be neglected.
- residual stresses at room temperature are significant.

Numerical calculations of crack propagation, taking into account residual stresses, load ratio and temperature effects give a fair estimate of the underclad cracks behaviors observed during testing.

Combining experimental and numerical results provides a good knowledge of real margins between the actual underclad crack propagation and the propagation that was calculated in past safety assessments.
It can be concluded that the actual propagations of underclad cracks will be very small or even negligible during the specified lifetime of the components.

1 INTRODUCTION

The reliability of a reactor pressure vessel is usually assessed using Fracture Mechanics Methodologies. Such analyses are performed by using conservative assumptions on material properties and fatigue crack propagation laws. In the case of cold underclad cracks in PWR nozzles it has been shown that no propagation of these cracks through the full thickness of the cladding is to be feared during 40 years of in-service conditions (Vagner et al, 1980).

With the aim of describing more accurately the actual in-service behavior of such cracks a fatigue program was undertaken on large specimens extracted from a full size nozzle containing actual embedded cracks or machined artificial defects (slots).

To be more specific, the objectives were to investigate the following points :
1) Is there an initiation time necessary before a cold crack begins to propagate under fatigue loading.
2) How will it propagate in both materials (stainless steel cladding and base metal SA 508 Cl3).
3) What are the effects of residual stresses existing in the base metal and the cladding on the crack propagation at R.T and 300°C.
4) How will the shape of the cracks change during cyclic loading.
5) Does the absence of oxidizing environment in the cold cracks reduce the crack propagation rate as compared to that in air environment.

Answering these questions enables the estimation of inherent margins in the safety analyses.

2 EXPERIMENTAL METHODOLOGY

2.1. Material

The large specimen tested were taken out of an actual SA 508 Cl3 nozzle containing cold cracks in the H.A.Z. under the three layers cladding 309L/308L. Chemical analyses and mechanical characteristics of the materials are given in TABLES I and II.

2.2. Laboratories - Testing machine - Specimens.

Tests were performed in two laboratories : "INSTITUT DE SOUDURE" and "CETIM" on 1000 kN servohydraulic testing machines at frequencies 0.5-1 Hz, at room temperature and 300°C. In this last case the temperature was kept constant (± 5°C) in the test zone (≈ 100 mm). Typical specimen geometries are given in Figure 1. The central part was taken out of an actual nozzle with 309L/308L three layers cladding. Heads were welded on these parts for gripping in the testing machines.
Two types of specimens were used :
- specimens with embedded cold underclad cracks in the H.A.Z.
- specimens with through thickness underclad cracks simulated by electro-erosion machined slots. The slots consisted in rectangular strips with a width of 0.3 mm.

TABLE I : CHEMICAL COMPOSITION OF THE MATERIALS INVESTIGATED

MATERIAL	C	S	P	Si	Mn	Ni	Cr	Mo	Cu	Co	V
A 508 Cl3 (nozzle)	.16	.006	.009	.280	1.31	.69	.13	.49	.06	.02	.01
AWS 308L cladding	.023	.011	.015	.830	1.41	10.3	19.97	.096	-	0.25	-

TABLE II : TYPICAL MECHANICAL PROPERTIES OF THE MATERIALS INVESTIGATED

MATERIAL	0.2% Yield Strength at R.T. (MPa)	Tensile Strength at R.T. (MPa)	Elongation (5d) at R.T. (%)	Reduction of Area at R.T.	CHARPY V Impact Strength at 0°C (J/cm²)
A 508 Cl3	508	634	21.8	67.5	119

2.3. Methodologies used to follow the crack propagation during fatigue testing

X ray examinations were used to follow the propagation of the embedded cracks. They were performed with the specimens loaded in tension in order to keep the crack open. Furthermore, special care was taken to localize the X ray sources in the plane of the crack and to avoid diffraction by using Pb screens.

A travelling microscope with a micrometer was used to follow the propagation of through thickness machined slots. Beach marks which appear when tests are interrupted were also used to measure the crack propagation during cyclic loading after the end of the tests.

2.4. Residual stresses measurements

Residual stresses measurements were performed on blocks machined out of the actual nozzle. The dimensions of blocks were similar to those of the central parts of the specimens. Two stress relaxation techniques were used :

- layer removal technique (Kume, 1974 - Schimmoeller, 1977) where a strain gage is stuck on one side of the block and the block is sliced from the opposite side in thin layers.

- removal of parts of blocks by machining with strain gages stuck on each blocks.

2.5. Test parameters

The tests reported consist mainly :
- in the simulation of the load follow (15 % - 100 %) transient performed at 300°C.
- in the simulation of the heat up/cold down transient performed at 300°C.
- in the simulation of cold hydrotest which was performed at R.T. by imposing a deformation measured by a strain gage located on the base metal in the vicinity of the crack, just under the cladding.

3 TEST RESULTS - COLD CRACKS BEHAVIOR

3.1. Fatigue crack initiation on defects

An important feature of the cold cracks behavior is that these defects do not propagate immediately upon the start of cyclic loading. During cyclic loading a period extending between $\frac{Nf}{4}$ and $\frac{Nf}{3}$ (where Nf is the number of cycle to complete failure) is necessary before crack propagation begins. This fatigue

crack initiation stage is neglected in safety analyses resulting in a noticeable underestimate of lifetime.

This fatigue crack initiation stage was evidenced by :
1) accurate radiographic examinations during interruption of tests.
2) beach marks resulting from interruption of tests.
3) detection of crack initiation by accoustic emission techniques substantiated also by SEM examinations of the fracture surfaces.
A good agreement (typically 15-20% of number of cycles) was found between the early growth detected by radiographic examinations, the apparition of beach marks on the fracture surface and accoustic emission.
It was found from accoustic emission measurements that crack initiation occured first in the base metal. A record of the summation of accoustic emission counts is presented in figure 2. During 10^5 cycles a significant accoustic emission occurs which is attributed to localized fatigue crack initiations on geometrical irregularities of the defect boundary. This emission decreases until 3 x 10^5 cycles when again a significant increase is observed. From X rays and SEM examinations, this increase can be related to fatigue crack initiation in the base metal. Then a new increase of accoustic emission can be related to crack initiation in the cladding.

3.2. Environmental effects

Cold cracks are originally embedded and a particular feature to be noted is that fracture surface aspect changes after the propagating crack has reached the free surface of the cladding. Before reaching the surface of the cladding, the fracture surface is not well defined and looks like fracture in vacuum or inert environment (Hudson, 1970), (Mahoney, 1974), (James, 1976/1987). Afterwards well defined striations immediately appear.
These two aspect are illustrated in figure 3.
Numerical analyses of results (see § 4) also evidence the different behaviors of crack propagation between actual embedded cracks without contact with external environment and through thickness machined slots in contact with air at 300°C.

3.3. Residual stress measurements

Residual stress fields obtained by both methods used are presented in figure 4. It is to be noted that :
1) the "block removal" technique provides residual stress values for isolated points which integrate the local stress field in a material finite element. Thus steep variations of the stress field or peak stresses are not well defined (e.g: base metal cladding interface). On the other hand the values measured out of such zones are reasonably accurate.

2) The layer removal technique provides the stress field in a nearly continuous manner and peak stresses can be measured, however this technique becomes inaccurate when changes in measured strains due to layering are small as is the case at some distance from the interface.
The residual stress fields measured in the welding direction (i.e. perpendicular to the defects) are in agreement with previous measurements on HAZ, after relieving at about 600°C.
(Kume et al, 1974) : σy = 80 to 180 MPa in the cladding
σy = -100 Mpa in the base metal
(Faure et al, 1985) : σy = 180 MPa in the cladding

(Schimoeller-Ruge, 1977) : σy = 200 to 400 MPa in the cladding
σy = - 50 to - 100 MPa in the base metal

In order to schematize this stress field for numerical analyses of the crack propagation, a two level simplified stress field was considered (figure 4).

Taking into account the accuracy of the two measurement methods used a simplified stress field was considered :

σy : + 200 MPa in the cladding
σy = - 100 MPa in the base metal

The stress field at 300°C was estimated considering the changes of output of heat resisting strain gages between R.T. and 300°C. The values measured near the interface were just opposite to the residual stress values measured at R.T. indicating that the residual stresses in the cladding and in the base metal are about cancelled by the effect of thermal expansion when heating up to 300°C. This result is in agreement with similar consideration (Rahka, 1978) on materials having difference in thermal expansion coefficients about 5×10^{-6}.

4 RESULTS AND ANALYSES OF FATIGUE CRACK PROPAGATION RESULTS

Numerical simulation of the crack propagation, begining after the crack initiation period have been performed in order to analyse the results. Such simulations provide a basis to estimate the margins inherent in the crack propagation computation of the safety analyses.

4.1. Main assumptions

The general procedure for crack propagation computations was as follow :
- for each case the crack is supposed to have already initiated and to propagate both in the base metal and the stainless steel cladding.
- the numerical simulation is performed by using upper bounds and lower bounds of crack growth rate data available in air available for the two materials. Two sets of reference curves were used. The first one is given in Table III. It was defined several years ago for the earlier analyses. The second set is based on many more data and corresponds to more recent developments in FCGR reference curves for austenitic stainless steels (James,1982) and low alloy steels (Eason et al, 1987) (Rungta et al, 1986). The coresponding published mean curves are given in Table IV. For the purpose of bounding crack propagations an arbitrary factor of two was applied to these curves to obtain rough estimates of upper bounds and lower bounds of FCGR. In fact both sets of reference curves are not very different. As the cladding FCGR curves were not given at room temperature for the first set of curves, they were deduced from the 300°C curves by applying a reduction factor of 2. For the second set the reduction factor, based on a more extensive set of data, was 1.65 (James, 1982).In both cases the FCGR of the base metal was unchanged at R.T (Eason, 1987).
- Stress intensity factors for elliptical cracks (case of embedded actual defects) and for through thickness machined cracks have been computed using the formulations given by (Tada, 1979). These formulations take also into account the proximity of the surface.

- It was assumed that in the case of embedded cold cracks which are nearly elliptical, the propagation on the long axis took place in the base metal. This was substantiated by examination of fracture surfaces (figure 5).

- The effects of residual stresses have been considered to be negligible at 300°C (see § 3.3.).

TABLE III : FIRST SET OF FATIGUE CRACK PROPAGATION CURVES USED FOR NUMERICAL SIMULATION

Cladding (300°C)	Upper bound	$da/dN = 7.5 \times 10^{-10} \left(\frac{\Delta K}{1 - \frac{R}{2}} \right)^4$ for all ΔK $da/Dn = 1.3 \times 10^{-10} \left(\frac{\Delta K}{1 - \frac{R}{2}} \right)^4$ for all ΔK (mm cycle) (MPa$\sqrt{m}$)
Cladding R.T.		$\pm$ 2 reduction by a factor of 2
A 508 Cl3 base metal 300°C - RT	Upper bound	$da/dN = 7.95 \times 10^{-9} \left[K_{max}(1-R)^{0.75} \right]^{2.93}$ for $\Delta K \leq 20$ MPa$\sqrt{m}$ $da/dN = 2.6 \times 10^{-8} (\Delta K)^{2.67}$ for $\Delta K > 20$ MPa$\sqrt{m}$
	Lower bound	$da/dN = 3.80 \times 10^{-9} \left[K_{max}(1-R)^{0.75} \right]^{2.93}$ for $\Delta K \leq 20$ MPa$\sqrt{m}$ $da/dN = 1.5 \times 10^{-8} (\Delta K)^{2.67}$ for $\Delta K > 20$ MPa$\sqrt{m}$

TABLEAU IV : SECOND SET OF FATIGUE CRACK PROPAGATION CURVE USED FOR NUMERICAL SIMULATION

Cladding 300°C (James, 1982)	Mean cuve	$\frac{da}{dN} = 3.232 \times 10^{-9} (\Delta K)^{3.3021}$ mm/cycle
Cladding R.T.	Mean cuve	Reduction factor of 1.65
A 508 Cl3 base metal 300°C-R.T. (Eason, 1987)	Mean cuve	$\frac{da}{dN} = 7.87 \times 10^{-8} 1 \left[\frac{\Delta K}{2.88 - R} \right]^{3.07}$

4.2. Results and analyses of tests on through thickness cracks at 300°C

A typical evolution of a fatigue crack propagation from a through thickness machined defect as a function of elapsed cycles is given in figure 6. Results of crack propagation calculations are also reported using the two sets of upper bound and lower bound reference curves. It appears that in both cases the hypotheses provide a correct prediction of crack propagation in the base metal and in the cladding : the propagations computed with the upper bounds and lower bounds curves of each set bracket the experimental results.

4.3. Results and analyses of tests on embedded cold cracks at 300°C

Examples of results of crack propagation from cold cracks, toward the cladding and in the base metal are shown in figure 7 and 8. Numerical simulation of crack propagations performed using the set of hypotheses in paragraph 4.1. are also reported. It appears that the crack propagations are clearly overestimated in the cladding with also a tendancy for overestimation in the base metal.

At this stage, taking also into account the aspects of fracture surfaces appearances, it can be assumed that there exists favourable environmental effects, i.e. FCGR is lower due to the absence of air or agressive environment in the embedded cold cracks. This was also observed by (Schijve 1978) for internal cracks in an aluminum alloy. (James, 1986) also considered such a possibility for internal cracks in structures.
In order to model this crack propagation behavior in a simple way, constant estimated reduction factors of 4 and 2 were applied to the FCGR in the cladding and in the base metal respectively. These values were substantiated by results of FCGR studies in vacuum on both materials and from several data reported in literature (Smith, 1969), (Cooke, 1975), (James, 1976-1988),(Mahoney 1974), (Bowen 1985).
Corresponding crack propagation calculations are presented in figures 9 and 10 where it is shown that these hypotheses provide a correct prediction of actual cold cracks behavior, the experimental behavior being now well bracketed by the upper bound and lower bound curves.

4.4. Results and analyses of tests on through thickness cracks at R.T. (effects of residual stresses).

Measurements have shown that residual stress levels are significant near the cladding-base metal interface (about 200 MPa tensile in the cladding and - 100 MPa compressive in the base metal).
Therefore their effect had to be assessed.
It can be assumed that the stress intensity factors mainly depend on the residual stress field applied on the crack length. The calculations of the static stress intensity factors in the cladding and in the base metal due to residual stresses are detailed in figure 11. These stress intensity factors are mainly negative in the base metal and positive in the cladding.
Considering K_{max} and K_{min} due to the loading it is possible to define (Parker, 1982) an effective load ratio for the base metal and the cladding :

$$R = \frac{K_{min}\ (\text{loading}) + K(\text{residual stresses})}{K_{max}\ (\text{loading}) + K(\text{residual stresses})}$$

- if $R \geq 0$ the effect of residual stresses is considered to be equivalent to a classical load ratio effect taken into account in crack propagation laws.

- if $R < 0$ only the positive part of the stress intensity factor is to be considered :

$$\Delta K_{effective} = K_{max}\ (\text{loading}) + K\ (\text{residual stresses}).$$
$$R = 0$$

An example of the differences between two calculations performed with and without taking into account residual stresses is given in figure 12. It appears that the difference is small in the cladding (load ratio effect). On the contrary the crack propagation in the base metal is overestimated when the residual stresses are not taken into account (crack closure effect).
Another example of numerical simulation of a spectrum loading test with constant maximum load and several load ratio is presented in figure 13 which shows that the model correctly predicts the crack propagation.

5 ASSESSMENT OF MARGINS IN THE SAFETY ANALYSIS

In the assessment performed in the past, the crack propagation of underclad cracks has been computed with conservative safety hypotheses :
- upper bounds of crack propagations laws in air environment have been used for both the base metal and the cladding

- fatigue crack initiation on the actual underclad defects has not been taken into account
- crack lengths have been corrected using Irwin's correction which accounts for plastic zone sizes at crack tips
- cold cracks which are elliptical have been considered as strip defects
- lower bounds of yield strengh and toughness of the materials have been used.

Figures 14 and 15 show actual crack propagation as well as that predicted either from a safety type analysis (case 1) and a realistic model taking into account the elliptical shape of defects and a favourable environmental effect (vacuum) and neglecting crack initiation time (case 2).
The margins can be evaluated by considering both ratios :

actual life/calculated life (case 1) : typically 10-15
actual life/calculated life (case 2) : typically 2-4

We can observe that considerable margins do exist between actual and calculated propagations using hypotheses of the safety analyses. Particularly the number of cycles to have the crack breaking through the cladding with the conditions of the safety analyses is lower than actual number of cycles for crack initiation from the defects.

6 CONCLUSIONS

An extensive program has been undertaken in order to study the initiation and fatigue crack propagation of both artificial (machined) through thickness underclad cracks and actual embedded underclad cracks.
Accurate crack growth measurements have been performed during the tests by means of radiographic, optical microscopy and SEM examinations.
Typical features of underclad crack behavior have been evidenced :
- a significant initiation period is necessary before the embedded cold cracks propagate like fatigue cracks.
- There are evidences that the absence of air or agressive environment in the embedded defects induces slower crack growth rates as compared with air conditions.

Last, fatigue crack propagation behavior of both types of cracks (machined or embedded) can be predicted with reasonable accuracy by using a model which mainly takes into account, the defect geometry, the residual stresses and the fatigue properties relevant to the actual environmental conditions (absence of air and humidity) for the crack in both SA 508 C13 base metal and the 309L/308L cladding.

All the results show that the hypotheses taken for the safety assessments performed until now were very conservative. These assessments had already led to conclude that the underclad cracks could not cross the cladding during 40 years of specified lifetime. We can now conclude that the actual crack propagation of underclad cracks in the affected components will be very small or even negligible during the 40 years lifetime.

REFERENCES

Vagner,J., Robisson,F., Slama,G., Bernard,J.L., Buchalet,C., Pellissier-Tanon,A.(1980). Methodology for acceptability analysis of underclad cracks in PWR components. AIEA Conference Vienna.

Kume, R., Obayashi, H., Naiki, T.,(1974).Internal stress in thick plates weld-overlaid with austenitic stainless steel. Trans.Japan Welding Society, Vol.5, N°1, 1974.

Faure,F.M., Legatt, R.H., Martin, B.A.(1985).Measurements of residual stresses in an austenitic ferritic transition. Int.Conf.on effects of fabrication

related stresses on product manufacture and performance. Cambridge U.K.
Schimmoeller, H.A., Ruge,J.L.(1977). Estimation of residual stress in reactor pressure vessel steel specimen clad by stainless steel strip electrodes. Residual stresses in welded constructions and their effects.International meeting of London.
Hudson, C.H., Seward, S.K. (1970). A literature review and inventory of the effects of environment on the fatigue behavior of metals. Engineering Fracture Mechanics, Vol.8.
Mahoney, M.W., Paton,N.E.(1974). The influence of gas environment on fatigue crack growth rates in types 316 and 321 stainless steels. Nuclear Technology, Vol.23.
James, L.A.(1976). Fatigue crack propagation in austenitic stainless steels, Atomic Energy Review, 14-1, pp 37-86.
James, L.A.(1987). Fatigue crack progagation of low alloy steel in a vacuum environment. EPRI report NP 5345 Research project 1325-14.
Rahka, K.(1978). Thermal and mechanical loads and arguments for the assessment of the size of initially tolerable defects in welded claddings. IEAE Technical meeting on time and load dependant degradation of pressure boundary materials, Insbruck.
James, L.A., Jones,D.P.(1982). Fatigue crack growth correlations for austenitic stainless steels in air. Predictive capabilities in environmentally assisted cracking, PVP Vo.19 ASME.
Eason,E.D., Andrew, S.P., Warbrodt, S.B., Gilman,J.D. (1987). Fatigue and corrosion fatigue data analysis using FATDAC. Transaction of the 9th International conference SMIRT, Vol.F, Lausanne.
Rugnta, R.Mindlin, H., Gilman, J.D.(1986). Application of EPRI data base on environmentally assisted cracking in the nuclear industry. Materials Performance, Nov. pp 43-52.
Tada,H.(1973). The stress analysis of cracks handbook. DEL Research corporation, Hellertown, Pennsylvania.
Schijve, J.(1978). Internal fatigue cracks are growing in vacuum. Engineering Fracture Mechanics, Vol.10, pp 359-370.
James, L.A.(1986). Fatigue-crack propagation behavior of steels in vacuum and implications for ASME Section XI crack growth analyses. PVP Vol.112, pp 99-14, ASME.
Smith, H.H, Shahinian, P., Achter, M.R.(1969). Fatigue crack growth rate in type 316 stainless steel at elevated temperature as a function of oxygen pressure. Transactions of the metallurgical society of AIME, Vol.245, May, pp 947-953.
Cooke, R.J., Irving, P.E., Booth, G.S., Beevers, C.J.(1975). The slow fatigue crack growth and threshold behavior of a medium carbon alloy steel in air and vacuum. Engineering Fracture Mechanics, Vol.7, pp 69-77.
Bowen, P., Knott, J.F.(1985). Effects of segregation and environment on fatigue crack growth at elevated temperature. Proc. 7th Int.Conf.on the strength of metals and alloys. Montreal, Pergamon Press, pp 1305-1310.
James,L.A.,(1988). Fatigue crack propagation behavior of type 316 stainless steel at elevated temperature in a vacuum. Int.J.Fatigue, January 1988.
Parker,A.P.(1982). Stress intensity factors, crack profiles and fatigue crack growth rates in residual stress fields, ASTM STP 776 pp 03-31.

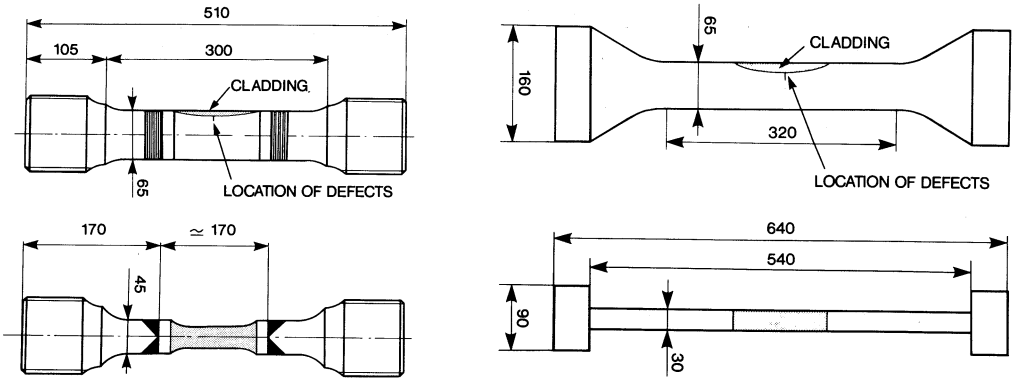

FIGURE 1 : Specimens geometries

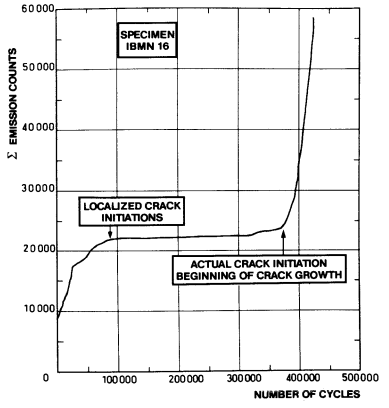

FIGURE 2 : Typical record of the summation of acoustic emission counts while testing an actual cold crack

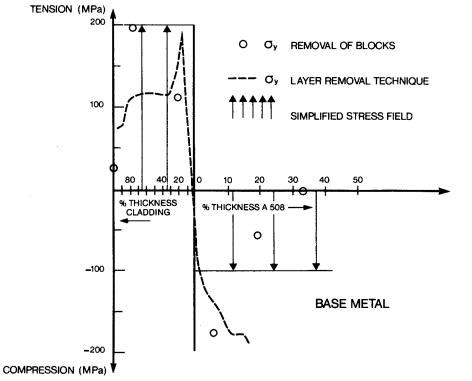

FIGURE 4 : Measurements of the residual stress field in the welding direction near the interface - Definition of a simplified field

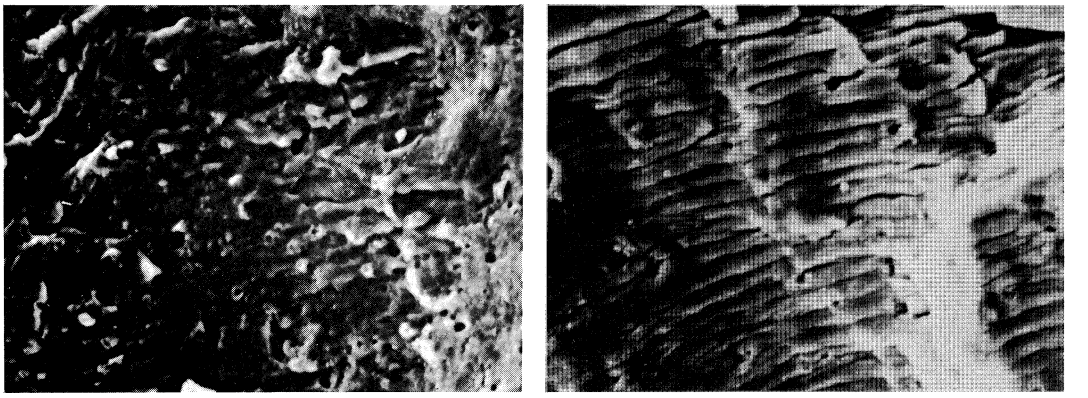

Embededd fatigue crack (a)

0,005 mm

Well defined striations (external fatigue crack)

0,005 mm

FIGURE 3 : Difference of fatigue surface aspect before (a) and after (b) the fatigue crack has reached the surface of the specimen

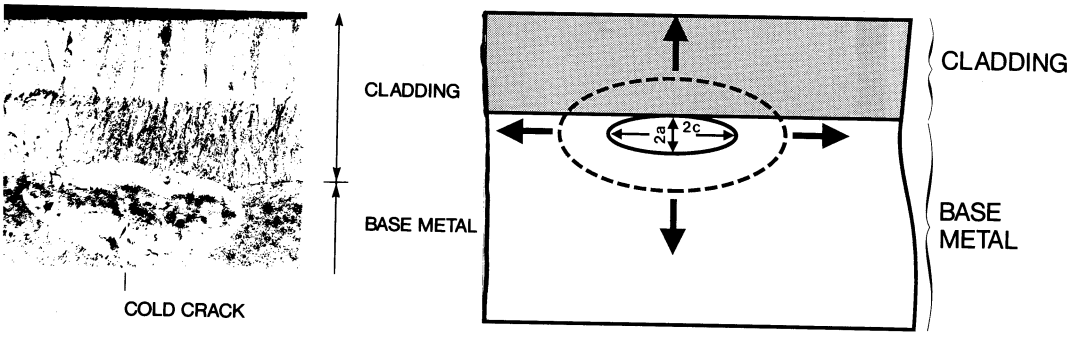

FIGURE 5 : Initial and final shapes of an embedded cold crack after fatigue testing

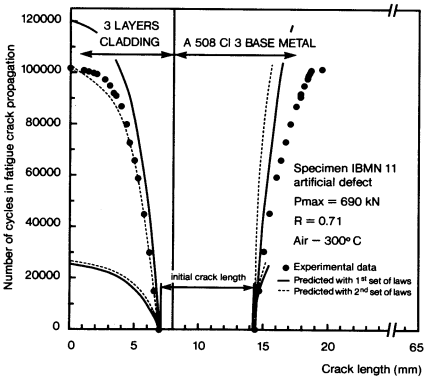

FIGURE 6 : Artificial underclad crack - Comparison between experimental and predicted crack propagation

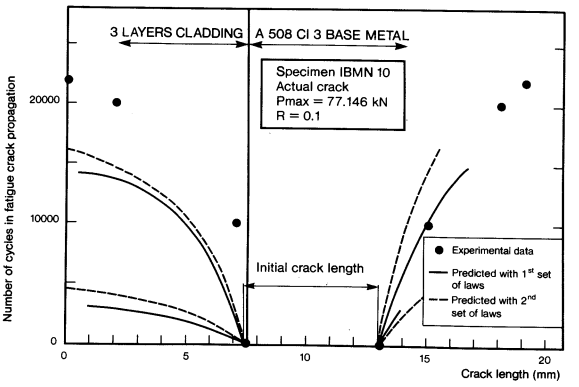

FIGURE 7 : Actual underclad crack - Comparison between experimental and predicted crack propagations

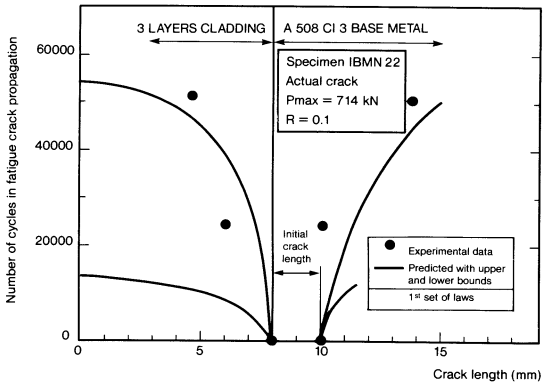

FIGURE 8 : Actual underclad crack - Comparison between experimental and predicted crack propagations

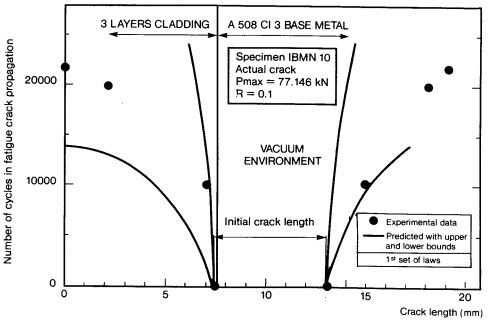

FIGURE 9 : Actual underclad crack - Comparison between experimental and predicted crack propagations (vacuum laws)

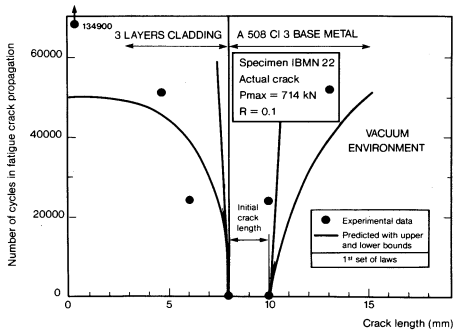

FIGURE 10 : Actual underclad crack - Comparison between experimental and predicted crack propagations (vacuum laws)

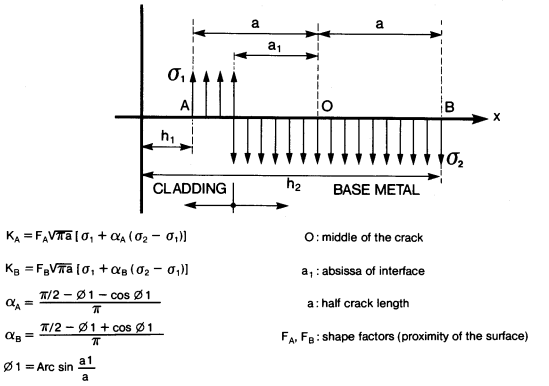

FIGURE 11 : Methodology for the stress intensity factors determination in a two levels residual stress field

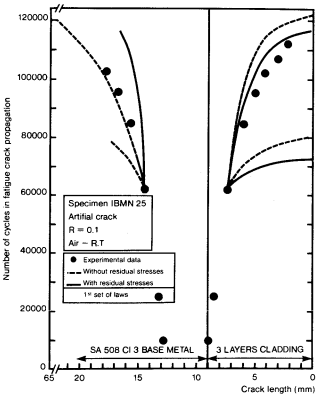

FIGURE 12 : Artificial underclad crack- Comparison between experimental and predicted crack propagations at R.T.

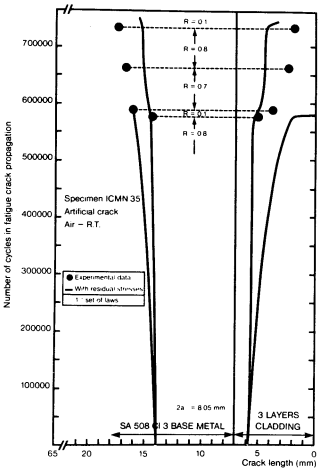

FIGURE 13 : Artificial underclad crack - Comparison between experimental and predicted crack propagations (complex loading at R.T.)

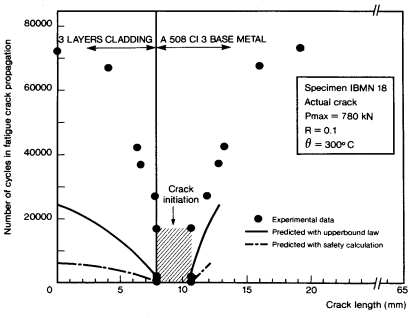

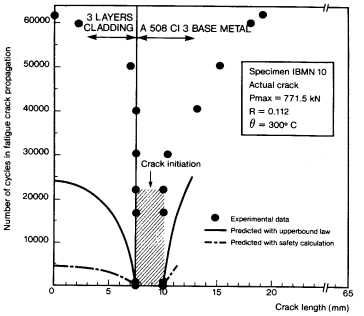

FIGURES 14-15 : Comparison between experimental and predicted crack propagation of actual underclad cracks using realistic crack propagations laws and safety hypotheses